Dynamics and interference of autoionizing wave packets

F. Texier and F. Robicheaux
Department of Physics, Auburn University, Auburn, Alabama 36849
(Received 5 August 1999; revised manuscript received 20 October 1999; published 1 March 2000)

We extend earlier theoretical work on the creation of autoionizing wave packets by a single laser pulse to the case where the autoionizing states are excited by two or more laser pulses. The calculations are performed using *R*-matrix methods combined with time-dependent multichannel quantum-defect theory. Atoms or molecules that are coherently excited into autoionizing states emit electrons in a series of pulses. We have found that the phase does not change rapidly across an electron pulse if the laser has little chirp. By choosing the delay between the two laser pulses, we can have the electron wave packets interfere. This interference can be exploited to partially control when the electron will be emitted and to partially control the time dependence of the channel into which it will be ejected. A comparison of the interference of different ejected wave packets gives information about the probability and phase to be initially excited into different channels.

PACS number(s): 32.80.Qk, 32.80.Dz, 32.80.Fb, 33.80.Eh

I. INTRODUCTION

Interferences produced by an electric or magnetic field separated into two coherent delayed components have important advantages in resonance spectroscopy [1]. The principle is applied in the optical Ramsey method (ORM): two identical laser pulses with a variable delay τ between them excite a quantum system in the coherent superposition $\psi(t)+\psi(t-\tau)$, where ψ is the time-dependent wave function for only one laser pulse. For each τ, the final electronic probability in the excited states constitutes one datum in the Ramsey signal. Due to the interference between $\psi(t)$ and $\psi(t-\tau)$, the signal oscillates as a function of the delay τ, and forms the so-called Ramsey fringes. The resolution of the fast sinusoidal oscillation of Ramsey fringes gives the final excited population [2].

When $\psi(t)$ is a coherent superposition of several successive Rydberg states, the time dependence of the wave-packet probability reflects the classical Kepler motion of the electron. The amplitude of the Ramsey fringes provides an interferential probe of this motion. If a part of the wave packet from the first pulse has returned to its initial position when the second pulse arrives, then the amplitude of the Ramsey fringes increases. The amplitude of the fringes is proportional to the absolute value of the autocorrelation function $\langle\psi(0)|\psi(\tau)\rangle$. Therefore ORM has been used for Rydberg dynamics in [3–5] for early works and in [6,7] for more recent examples. However, the information obtainable by this type of experiment can also be obtained from the usual continuous-wave photoabsorption versus energy experiment since the autocorrelation function may be obtained by Fourier transforming the energy-dependent cross section.

Different dynamical information may be obtained with a real-time measurement of the Rydberg probability [8] because the relative phases between the stationary components of the wave packet are not included in Fourier transforming the energy-dependent photoabsorption cross section. Real-time probabilities can be measured by the atomic streak camera [9]. In these experiments, the time dependence of the ejected electron flux is obtained with picosecond resolution. The ionizing electrons attracted by an electric field are accelerated through a slit before being quickly deflected by a voltage ramp and then detected in space, with the size of the deflection depending on when the electron passed through the slit.

In this paper, we consider an isolated quantum system excited by two delayed laser pulses into autoionizing Rydberg states; the generalization of the formalism to more laser pulses is straightforward. Coherent electronic wave packets that can interfere with each other are then created. Their dynamics of autoionization is followed in time by means of the outgoing electronic fluxes. Following in real time the autoionization process induced by two identical laser pulses is worthwhile because, for example, successive ionizing wave packets may have quite different behaviors that cannot be detected in ORM experiments because the signal is integrated over the real time. Part of the wave-packet phase information is physically accessible in real-time interference experiments. For a simple quantum system, we give analytical expressions for the wave packets and fluxes in the open channels. The wave packets produced by one laser pulse are expressed in terms of a spreading amplitude times a complex phase factor. By choosing the delay between the laser pulses, we make wave packets produced by different laser pulses interfere. The resulting measurable ionization flux is then related to the relative phase factor of interfering wave packets.

In Fig. 1, we plot the flux of the ejected electrons that were excited into autoionizing Rydberg states using three different laser pulse configurations. The ionization flux for excitation by a single laser pulse (solid line) consists of a first ionization burst ($t\approx 0$) coming from the electron being directly ejected after being excited, followed by bursts separated by the Kepler period that arise from the electron making 1 ($t\approx 6$ ps), 2 ($t\approx 12$ ps) or 3 ($t\approx 18$ ps) Rydberg oscillations before being ejected into the open channel. The dotted line gives the ionization flux when two laser pulses excite the autoionizing Rydberg states; the second laser pulse has roughly 1/2 of the intensity of the first pulse and has

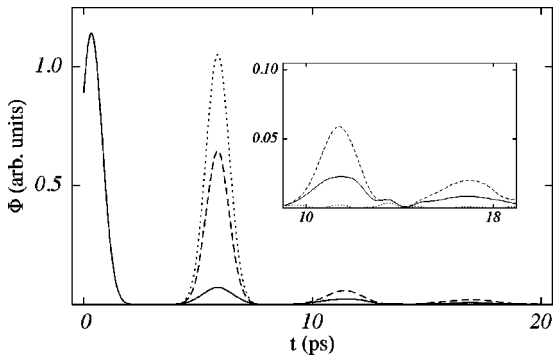

FIG. 1. Radial flux (as a function of time t) of the hydrogen molecule excited in autoionizing Rydberg states by one laser pulse (solid line) and by two coherent laser pulses separated by a delay τ close to the Kepler period (dotted and dashed line). When the delay τ is precisely fixed, the flux is obtained by a coherent superposition of the autoionization wave function created by each laser pulse (dotted line), while an incoherent summation is required when τ varies over a few laser periods. The first peak (solid, dashed and dotted lines) corresponds to the temporal density of probability for the direct ionization process. The later peaks (solid line) represent the flux for indirect ionization after successively 1, 2, and 3 Kepler periods. When the two laser pulses are used, the interference effect of ionization process after different Kepler period are manifested in all peaks (dotted line) after the initial one. For a particular relative phase between the two laser pulses (dotted line), the probability of ionization after 8 ps almost drops to zero when the intensity of the second laser pulse over the intensity of the first one is set equal to the probability for the quantum system in the closed Rydberg channel to be left in the closed channel after one scattering of the Rydberg electron to the ionic core.

been delayed by almost exactly one Rydberg period. For this case, each peak in the ionization flux after the initial one comes from a coherent superposition of two time-delayed bursts produced by the different laser pulses. The two laser pulses are separated enough in time for the first ionization burst to be ejected before the second laser pulse arrives, then no interference effect is expected in this burst. The interference effect, which appears in the second and later bursts (dotted line), increases the ionization probability in the second burst and almost cancels ionization in later bursts. This interferential control of the ionization dynamics is obtained for the particular value of the delay τ when the intensity of the second laser pulse over the intensity of the first one equals the probability of scattering from the closed channel into the open channel (both laser pulses have the same central energy E_0). Such intensities maximized the interference effect in each ionization burst of Fig. 1 because the interfering Rydberg wave-packet amplitudes are then roughly the same. The dashed line corresponds to the ionization flux where the delay between the laser pulses is averaged over one laser period: this can be experimentally realized by creating temporal oscillation of the optical path of one laser beam. The relative phase between interfering wave packets must then be averaged, and the ionization flux is then well represented by the incoherent summation (dashed line) of the ionization fluxes created by separated laser pulses. The phase control (dotted line) of the ionization dynamics then disappears (dashed line). The contrast between the dotted and the dashed lines illustrates the interference between the excitation caused by two laser pulses.

This example shows that a second perturbative laser pulse precisely delayed from a first one enables a control on the ejection time of the electron. Figure 1 manifests four important features of a typical Rydberg wave packet created by two coherent laser pulses separated by a precise delay τ close to the Rydberg period: (i) each laser pulse creates an initial electronic wave packet that is split into two coherent parts by scattering with the ionic core; after a few Rydberg periods the Rydberg motion is described by a multitude of coherent wave packets; (ii) each wave packet has a specific phase in the case of an unchirped laser; (iii) this phase and then the interference of wave packets created by the different laser pulses can be controlled by the small variation of the delay τ because the Rydberg period is much longer than the laser period; a much bigger variation of τ is necessary to change the dynamics of individual wave packets, (iv) by choosing the relative amplitude and delay of the laser pulses it is possible to modify the ejection time. For the multiopenchannels Mg case, we will show that it is also possible to control the ejection channel. Furthermore, it is possible to measure the relative phase of the successive electron pulses by varying the phase $E_0\tau$ between the laser pulses.

In the cases we consider, only one electron has an appreciable probability of being excited to Rydberg states. The nonexciting electrons with the nucleus constitute the core of the system. The core is in low excitation levels, so that outside a small core region the Rydberg electron is in a spherical potential. When the Rydberg electron is inside the core region, exchanges of energy and orbital momentum between it and the core are possible. Considering the small size of the core and the acceleration of the Kepler motion in this region, the scattering electron spends very little time inside the core; this time will be neglected compared to the time scale of the Kepler motion.

The time-dependent radial wave function for separated exciting laser pulses is obtained by a coherent superposition of the energy-dependent multichannel quantum-defect theory (MQDT) autoionization eigenstates multiplied by the temporal evolution phase factor and the amplitude of the laser electric field. The time-dependent wave functions are then superposed coherently to preserve the interference effects between wave packets created by different laser pulses. The multichannel quantum-defect theory (see [10] for stationary atomic examples) has been applied for a temporal description of the isolated quantum system, autoionized atoms [11,12], and molecules [13], for dynamics of two degrees of freedom in competitive autoionization predissociation in the hydrogen molecule [14] in a nonperturbative treatment, as well as for atomic autoionization in a static electric field [15] using parabolic coordinates instead of a spherical coordinate for the scattering electron.

As a preliminary illustration, we consider typical two-channel autoionizing systems excited by two identical laser pulses. For those systems, analytical formulas for the temporal radial fluxes characterize the role of the quantum and

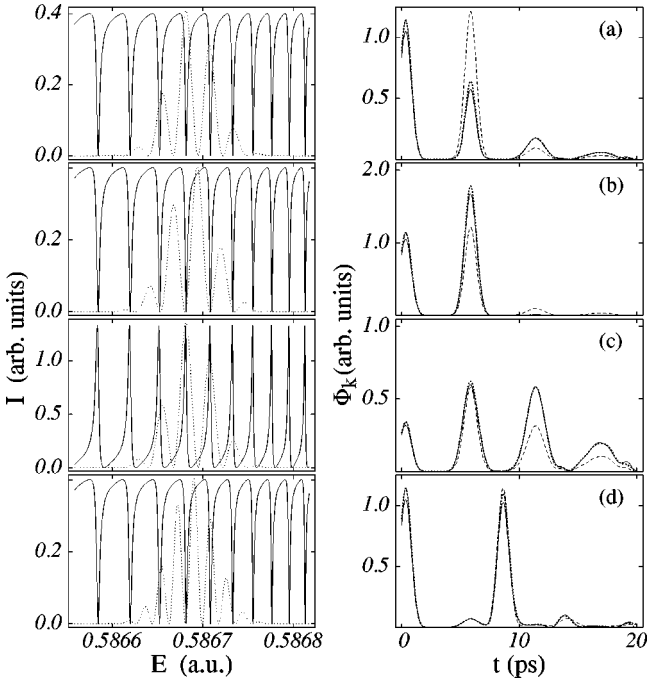

FIG. 2. Interferences of Rydberg wave packets. Left, photoionization cross section (solid line) and density of probability of finding a photon (dashed line) as function of the energy. Right, ionization fluxes $\Phi_k(r,t)$ at $r=1000$ a.u. as a function of time, calculated with the analytical formula of Eq. (3) (dotted lines), with an analytical formula without correlation between wave packets induced by different laser pulses (dashed lines), and by numerical calculation from Eqs. (2) (solid lines), (a) for two pulses delayed by $\tau = T(E_0) = 5.524\,313$ ps, (b) for $\tau = 5.524\,19$ ps, (c) for two pulses delayed by $\tau = T(E_0)$ and another quantum system with asymmetric autoionization profiles, and (d) for two pulses delayed by $\tau = 1.5T(E_0)$ $\psi(t)$ and $\psi(t-\tau)$ almost not interfering.

laser parameters in the dynamics of the wave packet. An application to atomic magnesium with a nonperturbative *R*-matrix calculation of the inelastic core scattering amplitudes shows the interference effects on partial ionization cross sections. Unless explicitly stated otherwise, atomic units will be used throughout this paper.

II. TYPICAL ONE CLOSED CHANNEL AUTOIONIZING SYSTEMS COHERENTLY EXCITED BY A SERIES OF LASER PULSES

This section presents the basic properties of autoionizing wave packets created by exciting a quantum system by two or more time-delayed coherent Gaussian laser pulses. For simplicity, we consider a two-channel quantum system with one closed channel coupled to one open channel, but the qualitative results may apply for more complex systems. The energy-dependent photoionization cross section consists of a regular series of resonances, such as in Fig. 2(a), left for the hydrogen molecule. The spacing and width of the resonances give respectively the period and lifetime of a wave packet in the closed channel. The coherent excitation of these resonances by each laser pulse creates localized electronic wave packets having a periodic motion in the closed channel before escaping in an open channel where they may interfere.

A. A two-channel quantum system

For a first physical example we consider the hydrogen molecule of Ref. [13], excited to the energies ~ 0.5865 to ~ 0.5868 a.u. above the fundamental state, between two ionization thresholds corresponding to the rovibrational quantum states $|N^+=0,v^+=2\rangle$ and $|N^+=2,v^+=2\rangle$ of the ionic diatomic core. N^+ (v^+) are the rotational (vibrational) quantum numbers of the core. In this energy range the rotation of the core is strongly coupled to the radial motion of the excited electron, and other couplings can be neglected in the first approximation. When the molecule is in the closed channel $|i\rangle = |N^+=2,v^+=2\rangle$, the Rydberg electron scatters once to the core within the Kepler period of ~ 5.52 ps. During this time the rotational energy of the diatomic core can be transferred to the Kepler motion with a probability $\sim 1/2$. The scattering amplitudes are given by the short-range scattering matrix

$$\mathcal{S}_{kk} = 0.708\,959 e^{-0.001\,397\,35 i\pi},$$
$$\mathcal{S}_{ki} = \mathcal{S}_{ik} = 0.705\,249 e^{-0.387 i\pi}, \quad (1)$$
$$\mathcal{S}_{ii} = 0.708\,959 e^{+0.227\,397 i\pi}.$$

$|\mathcal{S}_{ki}|^2$ is the probability that one Rydberg electron scattering to the core will change the quantum state of the core from state *i* where the complete system is bounded to state *k* where it is ionized. $|\mathcal{S}_{ii}|^2$ ($|\mathcal{S}_{kk}|^2$) is the probability of elastic radial scattering in the closed channel *i* (open channel *k*). The complex phase of $\mathcal{S}$ elements corresponds to twice the scattering phase shift of the radial wave function for the associated short-range process. The symmetry of $\mathcal{S}$ expresses the microreversibility of the scattering. The autoionization decay depends on the Kepler period and on the short-range scattering matrix elements between open *k* and closed *i* channels. The energy-dependent ionization cross section [Fig. 2(a), left, solid line] exhibits a series of Rydberg resonances with a window profile associated with a much bigger dipole amplitude $D_k = 1/\sqrt{3}$ in the open channel *k* than in the closed channel $D_i = 0$, due to the rotational inertia of the ionic core.

B. Real-time interference effects on photoionization induced by two identical laser pulses

Interesting interference effects are manifested when exciting the system with two identical laser pulses. The interference between two identical laser pulses modulates the amplitude of photon frequencies by a factor $1+e^{i\omega\tau}$, where ω is a frequency component and τ is the delay between laser pulses (see dotted lines Figs. 2(a)–2(d), left). In our example the laser intensity has a Gaussian profile, its central energy is $E_0 = 0.586\,687\,75$ a.u., and its full width at half maximum (FWHM) is set to 0.596 77 a.u. (1.12825 ps for temporal FWHM). The laser beam is split into two components of equal intensity but delayed by the time τ. Several autoionization resonances are excited around the central effective

quantum number $n^*=33.1224$, so that each laser pulse creates a Rydberg wave packet with a Kepler period $T(E_0)=5.524\,313$ ps. Because $1/\omega \ll T(E_0)$, a slight change of the delay τ will change the relative phase between wave packets from different laser pulses, but not their velocity. This is manifested by the large change in the photon distributions in Figs. 2(a) and 2(b), dotted lines, although τ has only been changed by $\sim 2\times 10^{-4}$ ps. The time-dependent wave function for the quantum system excited by two identical laser pulses is given by the coherent superposition

$$\Psi(t)=\psi(t)+\psi(t-\tau), \tag{2}$$

where $\psi(t)$ is the time-dependent wave function if only the first laser pulse excites the system. By choosing τ close to the Kepler period, Figs. 2(a)–2(c), we make wave packets of comparable amplitude interfere. Wave packets from the second laser pulse coincide in time and space with the first laser pulse wave packets that have one less closed channel scattering in their past.

Figures 2(a) and 2(b) differ only by a slight shift of τ, while (a) and (c) differ only by dipole amplitudes that are artificially changed for (c). If the two laser pulses were incoherent the flux of (a) and (b) should be obtained by the one laser pulse flux of Fig. 1(a) added to itself and translated in time by the Kepler period; this incoherent sum is plotted with the dashed line in (a)–(d), right. The difference between (a) and (b) comes from a different phase shift between interfering electronic wave packets; thus the phase of wave packets cannot be disregarded in the real-time measurements.

The time-dependent fluxes [Figs. 2(a)–2(c), right, solid or dotted line] present between $t=0$ and $t=20$ ps four ionization bursts separated by the Kepler period. The first burst (at time $t\approx 0.3$ ps) gives the direct ionization signal induced by the first laser pulse. It is the same in Figs. 2(a) and 2(b) and Fig. 1 because interference does not yet occur. However, the first burst differs in Fig. 2(c) because the dipole amplitudes have been artificially modified. In (a)–(c), the second burst (at $t\approx 5.8$ ps) corresponds to a coherent superposition of the first indirect ionization wave packet induced by the first laser pulse with the direct ionization wave packet induced by the second laser pulse; the third (fourth) burst corresponds to the interference of the second (third) indirect ionization wave packets from first laser pulses with the first (second) indirect one from second laser pulse.

The interferenc of the wave packets has a strong effect on the ionization flux, solid or dotted line in Figs. 2(a)–2(c), right; interferences are disregarded in the dashed lines, which correspond to an incoherent summation of the flux produced by each laser pulse. The comparison of dotted and dashed lines shows that the interference effect is generally different for each successive burst. In (a) τ equals the Kepler period $T(E_0)$, the interference is destructive for the second burst and constructive for the two latter ones, while the opposite effect is obtained in (b) where $\tau=T(E_0)-0.96\pi/E_0 \approx \tau$, E_0 being the central laser energy. For the same delay τ the interference in the second burst is constructive in (a) and neutral in (c). The interferences in the latter peaks are destructive in (a) and constructive in (c). In Sec. II D we show that the second burst intensity as a function of τ oscillates $\approx 180°$ out of phase with the latter bursts in the case of Figs. 2(a) and 2(b), while in case of Fig. 2(c) they oscillate $\approx 90°$ out of phase. In Sec. II D, we show that the relative phase of interference of the electronic peak at $\tau=T$ (5.5 ps) compared to that at $2T$ (11 ps) contains important information about the difference between direct and indirect ionization wave packets, which is mainly characterized by the phase of the profile parameter Q_{ik}.

In Fig. 2(d), right, the interferences are almost nonexistent because the wave packets excited by the two laser pulses almost do not overlap in time when $\tau=1.5T(E_0)$. The interference is not required before $t\approx 15-20$ ps, because we almost know with certitude which laser pulse has excited any electron detected.

Predictions can be made from the stationary Figs. 2, left. Energies that give ≈ 0.4 (nonresonant energies) for the cross section (solid line) contribute to the time-dependent excited wave function for short times, while resonant energies contribute for latter times. The radiative power spectrum (dotted line) is shifted in energy by a slight change of τ between (a) and (b), left. Then, in the stationary (a) left, more resonant energies contribute to the ionization process than in the case of (b), left, and the ionization should occur at the latter time for case (a). That is verified by the fluxes of (a) and (b), right.

C. Two-channel model

The fluxes of Fig. 2 are obtained from the coherent superposition $\psi(t)+\psi(t-\tau)$ of the time-dependent MQDT radial wave function $\psi(t)$ calculated as in previous works [11,13,14]. The photoionization process is described in a semiclassical formalism, with the photons represented by a classical oscillating electric field. The quantum system is assumed to be excited in the weak-field approximation by P Gaussian coherent laser pulses from a well-defined initial state of energy $E=0$ to the energies E around the central energy E_0.

The complex dipole amplitudes $D_k^-(E)$ can be expanded in an infinite series (see, for example, [11]), which decomposes the photoionization process into a series of ionization processes with specified travel in the different channels of the system. When there is only one closed channel i, each term of the series differs in the number n of scattering inward and outward in the closed channel. While traveling inward and outward in the closed channel the electron accumulates a phase shift from the Coulomb potential $2\beta_i(E)$, depending on the total energy E. $\beta_i(E)$ is related to the effective quantum number $\nu_i(E)=1/\sqrt{2(E_i-E)}$, where E_i is the threshold energy of the Rydberg equation by $\beta_i(E)=\pi(\nu_i(E)-\nu)$. The inelastic scattering at the core is given by the short-range scattering amplitudes in Eqs. (1). The energy derivative of the scattering phases corresponds to the duration of the process. The electronic scattering outside the core being much slower than the other elementary processes, the energy dependence of D_k is almost entirely due to $\beta_i(E)$.

We expand $\beta_i(E)$ to second order of the energy around E_0. The first derivative of $2\beta_i(E)$ with respect to E corre-

sponds to an elementary elastic scattering duration in the closed channel that equals the Kepler period; the second derivative gives the closed channel radial dispersion, which can be important as early as the first Kepler periods. Considering the fluxes of ionization probability at short distances (e.g., $r \approx 1000$ a.u.), the spreading of the wave packet in the Coulombic potential in the open channels will be neglected and then the radial phase $\varphi_k(r,E)$ is expanded to first order in E; the first derivative of $\varphi_k(r,E)$ with respect to E is the time required for the electron to travel from the core to the radius r. The time-dependent amplitude of the pth laser pulse is chosen to be the Gaussian $\epsilon_p \alpha_p^{-1} \exp[-(t-\tau_p)^2/(4\alpha_p)^2]$. Therefore the flux $\Phi_k(r,t)$ of probability of photoionization by channel k can be approximately expressed in terms of Gaussian spreading amplitudes $G_{n,p}(r,t)$, where p specifies the corresponding laser pulse, and n is the number of radial periods in the closed channel:

$$\Phi_k(r,t) = \left| 2\pi \mathcal{D}_k^- \right|^2 \left| \sum_{p=1}^{P} G_{0,p}(r,t) + Q_{ik} \sum_{n=1}^{\infty} \mathcal{S}_{ii}^{n-1} \sum_{p=1}^{P} e^{in(2\beta_i(E_0) - E_0 T_i(E_0))} G_{n,p}(r,t) \right|^2 . \tag{3}$$

where

$$Q_{ik} \equiv \mathcal{S}_{ki} \mathcal{D}_i^- (\mathcal{D}_k^-)^{-1},$$

$$G_{n,p}(r,t) \equiv \frac{\sqrt{\pi}}{\alpha_p \gamma_{n,p}} \exp\left[-\left(\frac{t - t_{n,p}(r)}{2\alpha_p \gamma_{n,p}} \right)^2 \right] e^{-iE_0[t - t_{n,p}(r)]}, \tag{4}$$

$$t_{n,p}(r) \equiv \mathcal{T}_k(r,E_0) + nT_i(E_0) + \tau_p ,$$

$$\gamma_{n,p} \equiv \sqrt{1 - \frac{in}{2\alpha_p^2} \frac{dT_i}{dE}(E_0)}.$$

The Rydberg period is $T_i = \partial 2\beta_i / \partial E$ and the travel time of the electron from the core to the radius r is $\mathcal{T}_k = \partial \varphi_k / \partial E$. The probability of detecting an electron has maxima at $t = t_{n,p}(r)$. The $t_{n,p}(r)$ is the cumulated travel time in closed and open channels added to the delay τ_p for the laser pulse p. τ_p is naturally defined as the time where the excitation by laser pulse p is maximum. The width of the direct ionization wave packets $G_{n=0,p}(r,t)$ is due in main part to the incertitude $\approx \alpha_p$ of the initial time of excitation by the laser pulse p and therefore the shape of the direct peaks in the flux of probability is close to that for the laser pulses. The parameter $\gamma_{n,p}$ arises from the dispersion and chirp of the wave packet in the closed channel due to the energy dependence of the Kepler period. The complex spreading factor $\gamma_{n,p}$ becomes important after a few periods n in the closed channel because the FWHM of the wave packet probability increases with n. Equation (3) indicates that detecting in real time simple autoionization fluxes created by two coherent excitations gives the opportunity to determine the phase and modulus of QDT parameters, as well as dipole transition amplitudes.

Equations (3) and (4) show that the amplitude for the electron to be at the distance r at the time t is a coherent superposition of complex Gaussian functions; the flux is very accurately approximated by the absolute value squared of this amplitude. An important feature of these formulas is that the complex Gaussians are multiplied for each orbit of the Rydberg electron in channel i by the overall phase factor $\exp[2i(\beta_i(E_0) - E_0 T_i(E_0)]$. Each time the electron elastically scatters from the core in channel i it accumulates a phase $\arg(\mathcal{S}_{ii})$ that is 2π times the quantum defect for channel i; at the same time, the amplitude of the Gaussian decreases by the factor $|\mathcal{S}_{ii}|$. Every Gaussian corresponding to an indirect process has an additional phase shift and amplitude factor from Q_{ik}; therefore Q_{ik} is a specific interference factor between direct and indirect Gaussians. The relative phase of interfering Gaussian wave packets can be measured by the resulting intensity as a function of the phase difference between the laser pulses. Q_{ik} is qualitatively equivalent to the q Fano parameter [16] to characterize the profile of the resonances in the ionization spectra. $|Q_{ik}|^2$ is the probability for the electron to be ejected in the first indirect peak divided by the probability to be ejected in the direct peak.

D. Interference effect on the probability to ionize in the successive bursts of the flux

To get strong interference effects between $\psi(t)$ and $\psi(t-\tau)$, we set the delay τ between the laser pulses to be close to the Kepler $T(E_0)$ period, according to the results in Fig. 2. In most experiments, the laser frequencies are much larger than the Rydberg frequency $T^{-1}(E_0) = 1/(\partial 2\beta/\partial E)(E_0)$. It is then possible by slightly changing the delay τ between the laser pulses,

$$\tau \equiv \tau_2 - \tau_1 = T(E_0) + \delta\tau, \quad \delta\tau \approx E_0^{-1} \ll T(E_0), \tag{5}$$

to study the interferences effects over a complete optical cycle, $\Theta = E_0 \tau / 2\pi$, of the laser. Such variations $\delta\tau$ of τ do not significantly change the the position $t_{n,p}(r)$ of the wave-packet probability $|G_{n,p}(r,t)|^2$ but do change its phase $-E_0(t - t_{n,p}(r))$; see Eqs. (4).

Because τ is close to one Kepler period [Eq. (5)] the nth peak in the ionization flux (Fig. 2, right) that is centered at $t = t_{n,p=1} = t_{n-1,p=2}$ is a coherent summation of the wave packet $G_{n-1,2}$ created by second laser pulse $p=2$ having $n-1$ scatterings in the closed channel, with the wave packet $G_{n,1}$ from first laser $p=1$ having n scatterings in the closed channel; see Eqs. (4). The successive bursts in the ionization flux will be identified by the growing integers m, with $m=0$ for the direct ionization first burst. The integral over the time of each burst gives the ionization probability P_m in the burst m. Analytical expressions for the ionization probability in each burst are obtained by integration of the flux over the duration of the burst.

$$P_{m=0}(\tau)=|2\pi\epsilon\mathcal{D}_k^-|^2\pi^{3/2}/\alpha_p,$$

$$P_{m=1}(\tau)=\sqrt{2}P_{m=0}\left[|Q_{ik}|^2+1+2\left|\frac{Q_{ik}}{\gamma_{1/2}}\right|\times\cos(\phi_{SQ}(Q_{ik})+\phi_{laser})\right], \quad (6)$$

$$P_{m\geqslant 2}(\tau)=\sqrt{2}P_0|Q_{ik}\mathcal{S}_{ii}^{m-2}|^2\left[|\mathcal{S}_{ii}|^2+1+2\left|\frac{\mathcal{S}_{ii}}{\gamma_{1/2}}\right|\cos(\phi_{SQ}(\mathcal{S}_{ii})+\phi_{laser})\right],$$

with

$$\phi_{SQ}(M)\equiv E_0T(E_0)-2\beta_i(E_0)-\arg\left(\frac{M}{\gamma_{1/2}}\right), \quad (7)$$

$$\phi_{laser}\equiv E_0\delta\tau,$$

and considering $\delta\tau$ small compared to the duration of the laser pulses. $\gamma_{1/2}=1.053\,02e^{-0.071\,108\,5i\pi}$ is the spreading factor of Eq. (4) for $n=1/2$; it modifies the probability of ionization only in the interference term.

The probability $P_{m=0}(\tau)$ for ionizing in the first peak has no dependence in the phase of the laser ϕ_{laser}, because it has been induced by only the first laser pulse. The latter probabilities $P_{m\geqslant 1}(\tau)$ oscillate sinusoidally with ϕ_{laser}. The phase of these sinusoidal oscillations depends on the phase accumulated by the electron in the closed channel. $P_{m=1}(\tau)$ is the only probability whose phase depends on the shape of the energy-dependent cross-section resonances through the parameter Q_{ik}. $P_{m\geqslant 2}(\tau)$ depend on quantum defects by the short-range scattering matrix S for the interference phase, and on dipole momenta for strength.

In Fig. 3, the ionization probabilities P_m $(0\leqslant m\leqslant 3)$ for the first four peaks in flux are plotted, as a function of the delay τ between the two laser pulses, over a complete optical cycle. (b)–(e) correspond to the ionization probabilities $P_{m=1}(\tau)$ for different values of the dipole matrix elements corresponding to four values of the Fano q parameter that characterizes four typical resonance profiles of the energy-dependent cross section: For (b) $q\ll 1$ corresponds to window resonances; for (c) $q\gg 1$ corresponds to Lorentzian resonances; for (d) and (e) it corresponds to asymmetric Fano profiles with $q\approx\pm 1$. The probabilities of ionization in $P_{m=1}(\tau)$ depend on the interference of the first indirect wave packet from the second pulse with the direct wave packet from the first pulse. Therefore the amplitude depends on the ratio Q_{ik} of indirect-direct ionization: Though this peak happens at short time, it contains information about all indirect processes. Q_{ik} in the second peak in the electron flux plays the role of the scattering matrix element $\mathcal{S}_{ii}$ in later peaks [plots (f) and (g)]. Those important quantum parameters can be estimated from experimental fluxes at different delays τ and real time t using Eqs. (6).

An important general feature for the two-channel system is established: P_1 oscillates as a function of τ in phase with P_2 and P_3 for Lorentzian peaks [Figs. 3(c), 3(f), and 3(g)] in the cross section, and 180° out of phase for window resonances [Figs. 3(b), 3(f), and 3(g)]. For asymmetric profiles,

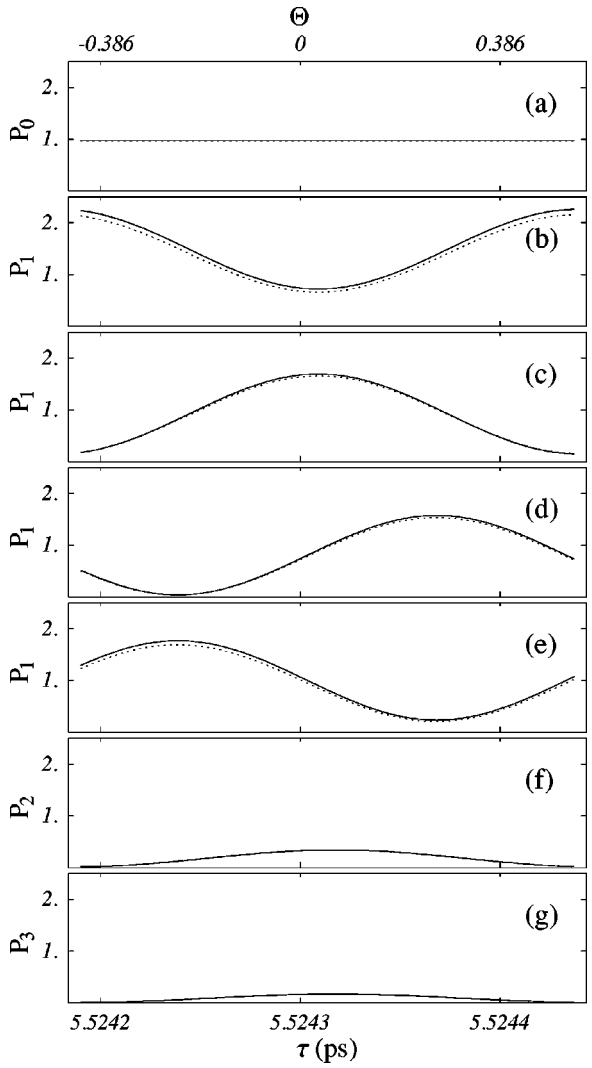

FIG. 3. Probability densities $P_m(\tau)$ in arb. units [Eq. (6)] of ionization in successive wave packets in open channel k coupled with a single closed channel i with a Kepler period $T(E_0)\approx 5.525$ (ps), for the four typical values of parameter Q_{ik}: $Q_{ik}=0.297\,217e^{-0.839\,645i\pi}$ for (a), (b), (f), (g) corresponding to the window resonances of the rotational autoionized hydrogen molecule. Curves (c)–(e) are for the same channel couplings as (b) but with changed dipole matrix elements so that $Q_{ik}=0.168\,225e^{0.160\,355i\pi}$ for (c), $Q_{ik}=0.984\,341e^{0.617\,696i\pi}$ for (d), $Q_{ik}=0.505\,289e^{-0.382\,304i\pi}$ for (e). The solid lines are from the analytical formulas, Eqs. (6) and (7), the dotted lines are from numerical calculations of the temporal flux. The phase, $\phi_{SQ}(M)-\phi_{laser}$, of the oscillation of P_m in radians divided by 2π at $\tau=5.5243$ ps is -0.469 for (b), 0.035 for (c), 0.264 for (d), -0.236 for (e), 0.066 for (f) and (g), $M=Q_{ik}$ for (b)–(e), and $M=S_{ii}$ for (f) and (g). P_1, the only probability P_m whose behavior depends on the profile of the resonances, oscillates as a function of the delay τ (or of the optical cycle $\Theta=E_0\tau/2\pi$) in phase with P_2 and P_3 for Lorentzian peaks (c), (f), (g) in the cross section, and 180° out of phase for window resonances (b), (f), (g). For asymmetric profiles, P_1 and $P_{2,3}$ oscillate 90° out of phase (d), (f), (g).

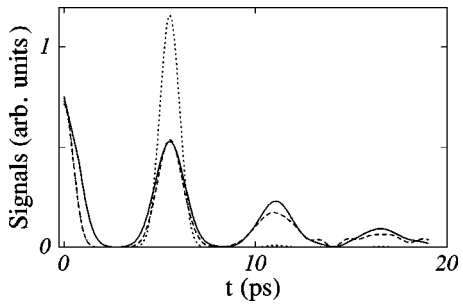

FIG. 4. Autocorrelation probability $|\langle\psi(t)|\psi(0)\rangle|^2$ (solid line) of the temporal wave function $\psi(t)$ for one laser pulse excitation, compared to the radial flux of probability (dashed and dotted lines) of the temporal wave function for two identical laser pulses delayed by τ. For the dashed line the delay τ between the two laser pulses equals the Kepler period $T(E_0)=5.52419$ ps [case of Figs. 2(b)], while for the dotted line $\tau=5.524\,313$ ps [case of Figs. 2(c)]. The three curves are rescaled and translated for the maxima of the first peak to be roughly the same. The autocorrelation measurement provides a temporal probability close to the autoionization flux only for particular values of the delay between the two laser pulses.

$q\approx\pm1$, P_1 and $P_{2,3}$ oscillate 90° out of phase [Figs. 3(d), 3(f), and 3(g) or 3(e), 3(f), 3(g)]. The medium value between the maxima of P_1 and minima gives $|Q_{ik}|$; the period gives its phase if we neglect the phase effect of the spreading factor $\gamma_{n,p}$. The amplitude effect of $\gamma_{n,p}$ can be deduced from P_2.

E. Comparison between autocorrelation and flux probabilities

The autocorrelation of the wave function is often used to describe the autoionization dynamics, though the associated experimental measurement is not in real time, and the signal may be obtained by Fourier transforming the stationary cross section multiplied by the energy density of photons. In ORM experiments, the temporal parameter that is varied is not the real time t but the delay τ between two identical laser pulses. As a function of τ, the total excited population, $2[|\langle\psi(0)|\psi(0)\rangle|^2+\mathcal{R}\langle\psi(0)|\psi(\tau)\rangle]$, oscillates with the laser period and forms the so-called Ramsey fringes. The first term $|\langle\psi(0)|\psi(0)\rangle|^2$ is constant, while the interferential term $\mathcal{R}\langle\psi(0)|\psi(\tau)\rangle$ causes the oscillation. The amplitude of the fringes varies with the Kepler period: If, when the second laser pulse reaches the quantum system, the wave produced by the first laser pulse has returned close to the core in the initial channel, the amplitude of the fringes is big because the total population in the excited state depends on the delay between the laser pulses. On the contrary, if the Rydberg wave packet is far from the core, the population in the excited state will not be affected by the second laser pulse. In the ORM, the spreading of the wave packets while traveling from the core to the flux detector is avoided.

In Fig. 4 is compared the autocorrelation probability, $|\langle\psi(0)|\psi(t)\rangle|^2$ (solid line) for the system to recover its initial state at time t, to the ionization fluxes for two close values of the delay τ between the two laser pulses: τ equals the Kepler period $T(E_0)=5.524\,19$ ps (dashed line) and $\tau=5.524\,313$ ps (dotted line). The autocorrelation measurements provide a rather good approximation of the ionization flux for the particular value $\tau=T(E_0)$ of the delay between the laser pulses. For a slightly different τ, one can no longer use the autocorrelation measurement (solid line) as an approximation of the ionization flux (dotted line). The ionization flux induced by to laser pulses allow us two study the coherence of autoionization in a two-dimensional temporal space, while only the delay between laser pulses can be varied for autocorrelation studies.

TABLE I. Orbital momentum quantum numbers, ionization potentials, and dipole amplitudes, for Mg.

$\|i\rangle\equiv\|l_c,s_c,j_c,Q,l_o,J\rangle$	I.P.	D_i
$\|1\rangle\equiv\|0,1/2,1/2,0,1,1\rangle$	0.0	0.658703211
$\|2\rangle\equiv\|0,1/2,1/2,1,1,1\rangle$	0.0	0.0
$\|3\rangle\equiv\|1,1/2,1/2,1,0,1\rangle$	0.162522	0.820531013
$\|4\rangle\equiv\|1,1/2,1/2,1,2,1\rangle$	0.162522	0.26675359
$\|5\rangle\equiv\|1,1/2,3/2,1,0,1\rangle$	0.162939	−1.16040609
$\|6\rangle\equiv\|1,1/2,3/2,1,2,1\rangle$	0.162939	−0.377246545
$\|7\rangle\equiv\|1,1/2,3/2,2,2,1\rangle$	0.162939	0.0

III. APPLICATION TO MAGNESIUM

In the preceding sections the interference between time-delayed ionizing wave packets has been discussed in real time for simple two-channel cases. In particular, interference between direct and indirect ionization wave packets' affects the behavior of the wave packets' probability P_1 of Figs. 3(b)–3(e) plotted as a function of the delay τ between the creation time of the wave packets by the two laser pulses. In the stationary cross section the competition between direct and indirect ionization appears in the profile of the resonances and Figs. 3(b)–3(e) correspond to four typical profiles obtained by artificially changing the value of the dipole amplitudes in closed and open channels. A more complicated autoionization system provides a natural set of dipole amplitudes and thereby a physical situation to study such dynamical effects of the resonance profile in the partial cross sections.

We consider the ionization process in atomic magnesium excited from the $3s^2$ ground state. There are three relevant core states of Mg^+ ($3s_{1/2}$, $3p_{1/2}$, and $3p_{3/2}$) in the energy range of interest to us. The autoionization process is described in seven channels coupled in the jQ scheme [17,11]. The orbital l_c and spin s_c momentum of the core are first coupled together to give the total angular momentum j_c of the core, which is coupled to the spin s_o of the outer electron to give Q. The angular momentum Q is coupled to the orbital angular momentum of the Rydberg electron, l_o, to give the total angular momentum J. Channel quantum numbers and ionization thresholds are given in Table I.

Mg is excited between the $3p_{1/2}$ ($l_c=1$, $j_c=1/2$) and the $3p_{3/2}$ ($l_c=1$, $j_c=3/2$) thresholds, so that the first four channels ($i=1-4$) are open, and some Rydberg states excited in closed channels $i=5-7$ give wave packets with identical Kepler period. The laser excitation initially preserves the spin coupling; therefore channels $|2\rangle$ and $|7\rangle$ that correspond

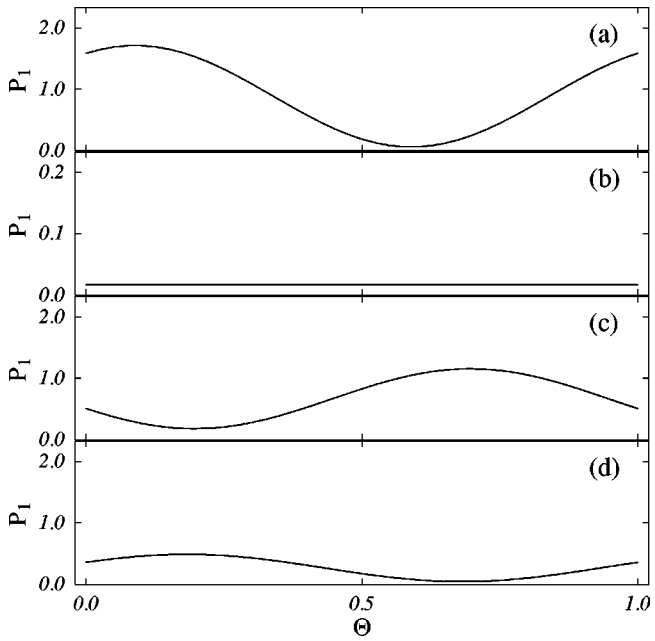

FIG. 5. Probability density P_1 (arb. units) [Eq. (6)] for Mg to ionize in each open channel with the second burst in the ionizing flux. Mg is excited by two identical laser pulses separated by the delay τ. As in Figs. 3, the electronic wave packet has a Kepler motion in only one closed channel i, with the period $T(E_0) \approx 5.525$ (ps), before leaving the system in one of the four open channels k. The phase $\phi_{SQ}(Q_{ik}) - \phi_{laser}$, of the oscillation of P_m in radians divided by 2π at $\tau = 5.5243$ ps is 0.410 for (a), undetermined for (b), -0.197 for (c), and 0.318 for (d). The sinusoidal behavior of the probability P_1 (plotted as a function of the optical cycle of $\Theta = E_0\tau/2\pi$ of the laser pulses) is an effect of the interference of direct and indirect ionization packets: (a) in channel $k=1$, (b) $k=2$, (c) $k=3$, (d) $k=4$ (see Table I). The interference differs in each open channel; therefore a selection of the ionized quantum states is enable by the choice of the delay τ.

to triplet coupling are not directly excited ($D_i = 0$ in Table I).

The delay between the two laser pulses is set to be equal to the Kepler period. Therefore the direct ionizing wave packet induced by the second laser pulse interferes with the first indirect wave packet induced by the first laser pulse. The partial ionization fluxes, like the two-channel system, exhibit successive peaks. The ionization probability in the successive peaks is given by the P_m of Eqs. (6). We focus on the ionization in the second peak (given by P_1), because this peak shows the interference between directly ejected electrons and those bound to the atom for only one period. The first peak is independent of the presence of the second laser pulse [see $P_{m=0}$, Eqs. (6)].

The probability of ionizing by channel $i = 1-4$ in peak P_1 is plotted in Figs. 5(a)–5(d) versus the optical cycle Θ (proportional to the relative phase of the laser components). This seven-channel case shows similar interferential behaviors as in the two-channel case [Figs. 3(b)–3(e)]. The sinusoidal oscillation of P_1 has different phase and amplitude in each open channel. In (a), (c), and (d) P_1 oscillates with Θ, but not in (b), because there is no direct ionization in the corresponding triplet channel. P_1 of Fig. 1 oscillates nearly in phase with P_1 of (d) and roughly 180° out of phase with P_1 of (c). The delay between the two laser pulses fixes the value of Θ and makes possible a level of control into which channel the Mg will ionize: $\Theta \approx 0.7$ almost cancels the ionization in channel $|1\rangle$ and $|4\rangle$ (see Table I) but maximizes the ionization in channel $|3\rangle$, whereas $\Theta \approx 0.2$ almost cancels the ionization in channel $|3\rangle$ but increases the ionization in channels $|1\rangle$ and $|4\rangle$.

IV. CONCLUSION

We have studied interference effects in autoionization processes for typical simple quantum systems and for atomic magnesium. Interference effects occur between Rydberg wave packets induced by coherent time-delayed laser pulses. Each wave packet has a definite phase and amplitude that is given in Eqs. (4). In this work, the interference effects have been studied in a two-dimensional temporal space, the real time t and the delay τ between two coherent excitations; the delay τ controls the relative phase of interfering wave packets. The coherence effects are time-dependent and the time-dependent wave function or flux allows us to identify the elementary processes that control the interferences at different times. A detailed comparison with autocorrelation measurement has been done. Because the physical process that is directly described by the autocorrelation function is not the autoionization process itself and because only the delay τ is a variable, less information can be obtained and the information is not straightforwardly related to autoionization processes.

We have used the time-dependent wave function to obtain an approximate analytical formula for temporal ionization flux induced by coherent time-delayed laser pulses. This enables us to characterize the role of the phase of the Rydberg wave packets as well as the dynamical effects of different stationary parameters, such as the q profile parameter of Fano. Numerical and approximate analytical formula results are in good agreement and are not limited to two laser pulses.

The variation of two independent temporal parameters, the real time t, and the delay τ between the laser pulses, provides a set of interesting interference effects between electronic wave packets. As a worthwhile consequence, the interference effects make possible a selection of the final ionized quantum states of the system by the choice of both the real time and the delay between the two laser pulses.

Ionizing wave packets created by an unchirped short laser have, in our examples, a well-defined relative phase that can be measured in real-time experiments where autoionizing wave packets interfere. The phase of the ejected electronic wave packets depends on the photoionization process; more precisely, the phase is related to the scattering and dipole matrix elements; therefore interference of autoionizing wave packets provides worthwhile phase information on the stationary wave function of the autoionizing quantum system.

ACKNOWLEDGMENTS

It is a pleasure to acknowledge discussions with L. D. Noordam and C. W. Rella. This work was supported in part by the NSF.

[1] N. F. Ramsey, Phys. Rev. **76**, 1 (1949).
[2] M. A. Bouchene, V. Blanchet, C. Nicole, N. Melikechi, B. Girard, H. Ruppe, S. Rutz, E. Schreiber, and L. Wvste, Eur. Phys. J. D **2**, 131 (1998).
[3] N. F. Scherer, R. J. Carlson, A. Matro, M. Du, A. J. Ruggiero, V. Romero-Rochin, J. A. Cina, G. R. Fleming, and S. A. Rice, J. Chem. Phys. **95**, 1487 (1991).
[4] L. D. Noordam, D. I. Duncan, and T. F. Gallagher, Phys. Rev. A **45**, 4734 (1992).
[5] B. Broers, J. F. Christian, J. H. Hoogenraad, W. J. van der Zande, H. B. van Linden van den Heuvell, and L. D. Noordam, Phys. Rev. Lett. **71**, 344 (1993).
[6] D. W. Schumacher, B. J. Lyons, and T. F. Gallagher, Phys. Rev. Lett. **78**, 4359 (1997).
[7] C. Trump, H. Rottke, and W. Sandner, Phys. Rev. A **59**, 2858 (1999).
[8] G. M. Lankhuijzen and L. D. Noordam, Phys. Rev. Lett. **76**, 1784 (1996).
[9] R. R. Jones and L. D. Noordam, Adv. At., Mol., Opt. Phys. **38**, 1 (1996).
[10] M. Aymar, C. H. Greene, and E. Luc-Koenig, Rev. Mod. Phys. **68**, 1015 (1996).
[11] F. Robicheaux, and W. T. Hill III, Phys. Rev. A **54**, 3276 (1996).
[12] H. H. Fielding, J. Chem. Phys. **106**, 6588 (1997).
[13] F. Texier and Ch. Jungen, Phys. Rev. A **59**, 412 (1999).
[14] F. Texier and Ch. Jungen, Phys. Rev. Lett. **81**, 4329 (1998).
[15] F. Robicheaux and J. Shaw, Phys. Rev. Lett. **77**, 4154 (1996).
[16] U. Fano, Phys. Rev. **124**, 1866 (1961).
[17] M. D. Lindsay, C.-J. Dia, T. F. Gallagher, F. Robicheaux, and C. H. Greene, Phys. Rev. A **46**, 3789 (1992).